

ZeroFlood: A Geospatial Foundation Model for Data-Efficient Flood Susceptibility Mapping

Hyeongkyun Kim^a and Orestis Oikonomou^{b,c}

^aGerman Aerospace Center (DLR), Remote Sensing Technology Institute, Oberpfaffenhofen, Germany

^bETH Zurich, Seminar for Applied Mathematics, Zurich, Switzerland

^cETH AI Center, Zürich, Switzerland

Abstract

Flood susceptibility mapping (FSM) is vital for disaster prevention but remains challenging in data-scarce regions where hydrodynamic models require dense geophysical inputs. This work introduces ZeroFlood, a geospatial foundation model framework for data-efficient FSM. The approach fine-tunes Geospatial Foundation Models (GFM) with Thinking-in-Modality (TiM) reasoning, enabling flood prediction from basic Earth observation data such as Sentinel-1 or Sentinel-2 imagery. Using paired EO and simulated flood maps from data-rich regions, ZeroFlood bridges data availability gaps through cross-modal representation learning. Experiments with TerraMind and Prithvi GFM show that TiM enhances model robustness, with the TerraMind-Large configuration achieving an F1 score of 67.21. The results demonstrate the feasibility of foundation-model-based FSM as a scalable and data-efficient solution for flood risk management.

1 Introduction

Floods are among the most frequent and devastating natural disasters worldwide, causing significant loss of life, economic damage, and long-term social disruption [2, 22, 27]. Effective flood susceptibility mapping (FSM) plays a crucial role in disaster avoidance, urban planning, and climate adaptation. However, traditional FSM approaches, typically based on hydrological and hydrodynamic simulations, require extensive high-quality input data such as digital elevation models, precipitation records, land cover, and river network information [8, 23]. These models, while physically interpretable, are computationally expensive and difficult to deploy in data-scarce or rapidly changing environments.

A major challenge therefore lies in developing data-efficient FSM methods that can generalize to regions with limited or missing geophysical information. Many flood-prone areas, particularly in developing regions, lack labeled data or calibrated hydrological simulations, hindering large-scale or real-time applications.

To address this limitation, we propose ZeroFlood, a geospatial foundation model framework designed for flood susceptibility mapping under limited data availability. ZeroFlood leverages Geospatial Foundation Models (GFM) pre-trained on large scale Earth observation (EO) datasets and applies Thinking-in-Modality (TiM) reasoning to infer flood susceptibility directly from unimodal inputs such as Sentinel-1 or Sentinel-2 imagery. This approach bridges data-rich and data-scarce regions, enabling FSM with minimal local resources while maintaining model robustness. The main contributions of this work are as follows:

1. Introduction of a geospatial foundation model based framework for data-efficient Flood Susceptibility

Mapping (FSM) that integrates Earth Observation (EO) data and flood simulation information.

2. Demonstration of TiM reasoning as an effective mechanism to enhance cross-modal understanding and compensate for missing data modalities.
3. Empirical validation showing that fine-tuning Geospatial Foundation Models (GFM) can achieve competitive flood mapping performance using only unimodal EO inputs.

This research extends the authors' award-winning project recognized by the European Space Agency (ESA) and IBM under the BlueSky Challenge ¹, emphasizing the broader potential of foundation models in geospatial and environmental applications.

2 Related Work

Simulation Model for FSM. Hydrological and hydrodynamic models play an important role in identifying flood-prone areas through physics-based simulations [23]. Recent research has introduced several models, such as HEC-RAS, Delft3D, InfoWorks ICM, LISFLOOD-FP, and CaMa-Flood, that simulate water flow and inundation using high-resolution digital elevation models (DEMs), precipitation, land use, and river network data [3, 8, 19, 25]. While these models provide accurate and physically interpretable results, they require extensive, high-quality input data and significant computational resources, which can limit their application in data-scarce or rapidly changing regions [1, 18]. Studies highlight that the performance of

¹<https://huggingface.co/spaces/ibm-esa-geospatial/challenge>

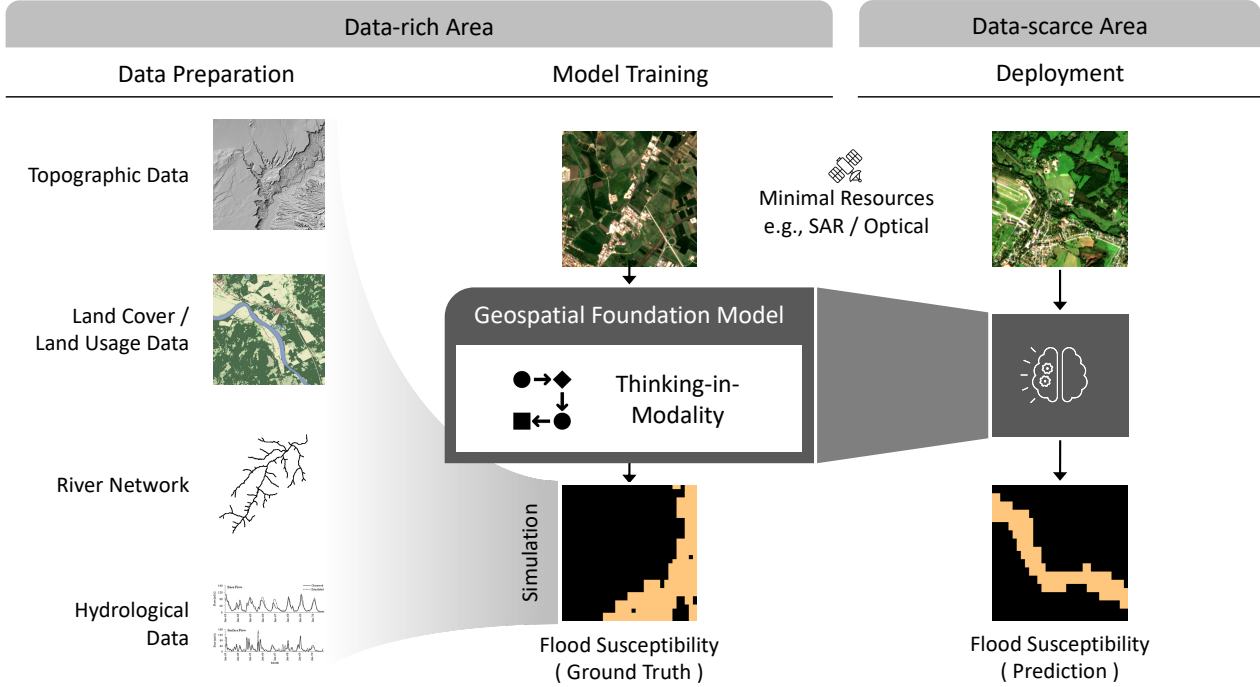


Figure 1 ZeroFlood framework for generating flood susceptibility maps in data-scarce regions using Geospatial Foundation Models (GFMs). Training data from data-rich areas are used to fine-tune large-scale GFMs. The Thinking-in-Modality (TiM) process is applied during fine-tuning and inference to compensate for missing modalities and enhance model performance.

simulation models is inherently constrained by the quantity and quality of input data, and large-scale implementations are often hindered by the trade-off between computational speed and accuracy [31]. This dependency motivates learning-based approaches that infer flood susceptibility directly from remote-sensing observations, reducing reliance on dense physical inputs.

Machine Learning for FSM. Unlike physics-based simulation models, ML approaches can learn complex and nonlinear relationships from diverse data sources, reducing the dependency on explicit physical modeling. Traditional ML methods, such as Support Vector Machines, Random Forests, and Ensemble models, have demonstrated high predictive accuracy [17, 20, 24]. More recently, deep learning methods, including MLP, CNN, and RNN architectures, have advanced the extraction of spatio-temporal features and improved model robustness and scalability [7, 11, 14]. Nonetheless, their performance still relies on the availability of sufficient and diverse training data, as they are typically trained for a specific downstream task. Therefore, data dependency remains a key challenge for deployment in data-scarce regions [9].

Geospatial Foundation Models (GFMs). GFMs are large-scale pre-trained models to unify sensing modalities and enable general-purpose downstream adaptations. They are built on diverse geospatial datasets, including optical, radar, and multispectral imagery, [16, 28]. To overcome label scarcity, GFMs typically leverage self-supervised learning techniques such as Masked Autoencoders, Contrastive Learning, and Self-distillation [5, 12,

13, 21, 26]. Owing to their generalized geospatial representations, GFMs demonstrate strong performance across various downstream tasks under low-data regimes, making them ideal for flood management applications in data-scarce environments [6, 15]. While multimodal and cross-modal approaches are becoming increasingly common for extensive feature representations [13, 28, 30], the practical applications of GFMs for flood-related tasks remain an open research problem. This motivates our use of a GFM backbone with TiM reasoning in Section 3

3 ZeroFlood Framework

The proposed ZeroFlood Framework consists of three main phases. i) Preparing a training dataset from a data-rich region. ii) Training a Geospatial Foundation Model (GFM) using the Thinking-in-Modality (TiM) approach. iii) Deploying the model to a data-scarce region for flood susceptibility mapping.

3.1 Combining Earth Observation with Flood Simulation Data

Flood susceptibility mapping typically requires multiple data sources, such as topography, hydrology, and land use information, which are often unavailable in data-scarce regions. In contrast, Earth Observation (EO) data, particularly optical and radar imagery, are widely available and mostly open-access [10, 32]. Therefore, we aim to train a Geospatial Foundation Model to learn from EO data and infer flood susceptibility directly from them.

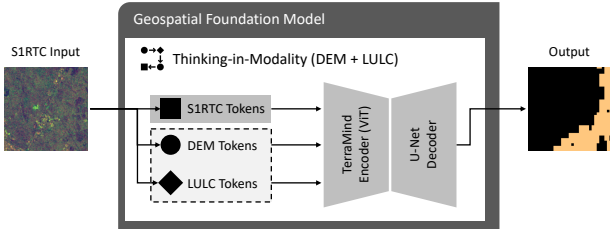


Figure 2 Illustration of the Thinking-in-Modality (TiM) process within a Geospatial Foundation Model. The process leverages information from additional modalities through pre-trained tokenizers trained on large-scale, multimodal geospatial datasets.

To achieve this, we sample a pair of EO imagery and simulated flood-susceptible mask. These datasets are processed and aligned to fit the input requirements of the model. Detailed descriptions of the datasets are provided in Section 4.1.

3.2 Thinking-in-Modality (TiM)

We focus on data- and resource-efficient flood susceptibility mapping. To this end, we use a unimodal and relatively small training dataset while maximizing model performance through transfer learning. Specifically, a pre-trained Geospatial Foundation Model, trained on large-scale multimodal EO data, is fine-tuned on our task-specific dataset. During fine-tuning and inference, we apply the Thinking-in-Modality (TiM) procedure to enhance model reasoning. TiM is inspired by the chain-of-thought strategy used in large language models [29], and was first demonstrated in the Geospatial Foundation Model *TerraMind* [13]. This model is trained on diverse multimodal datasets, allowing it to represent and reason across different EO data modalities within a shared token space. As illustrated in **Figure 2**, even when only unimodal data are available, the TiM procedure enables the model to generate complementary modality tokens, effectively enriching data representation. This mechanism helps mitigate the limitations of data heterogeneity and small training samples, improving the robustness of flood susceptibility prediction in data-scarce regions.

4 Experimental Setup

4.1 Dataset

Earth Observation Dataset. For spaceborne optical and radar imagery, we use the multimodal EO dataset *TerraMesh* [4]. *TerraMesh* provides five EO modalities with global coverage and precise spatial alignment across modalities. This study employs Sentinel-2 L2A and Sentinel-1 RTC products to represent the optical and SAR modalities, respectively. The Sentinel-2 L2A data include atmospheric correction, while the Sentinel-1 RTC data are terrain-corrected to ensure radiometric and geometric consistency.

Flood Simulation Dataset. For flood susceptibility

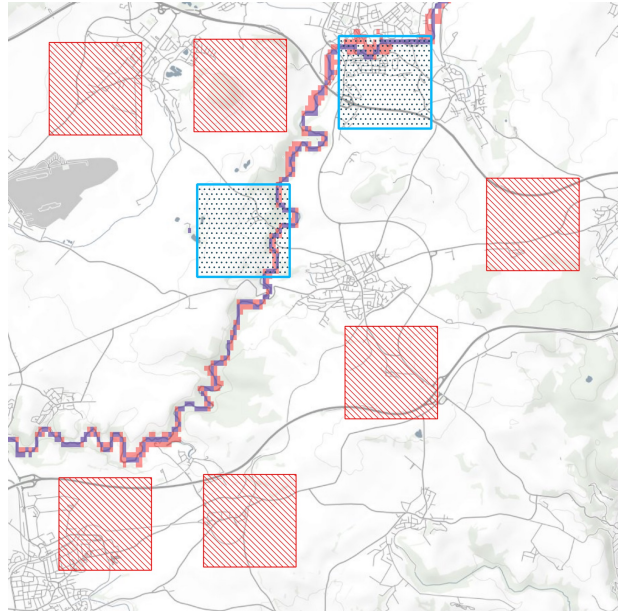


Figure 3 Example of overlap between TerraMesh samples and flood simulation data. Flood simulation data (red pixels) and permanent water bodies (blue pixels) are shown along river networks. Rectangular grid boxes represent sample regions extracted from TerraMesh. Boxes meeting the data-quality criteria are shown in blue; otherwise, they are shown in red.

masks, we use the river flood hazard data set for Europe and the Mediterranean basin simulated by the *LISFLOOD-FP* [8]. This provides inundation information for approximately 329,000 km of river networks for six flood return periods. We use 100-year return period maps as a flood susceptibility reference in our experiments.

As illustrated in **Figure 3**, TerraMesh and *LISFLOOD-FP* cover different geographical regions. Therefore, we identified overlaps and informative areas according to the selection policy described in **Algorithm 1**. Consequently, a total of 314 samples were generated and divided into training (186), validation (62), and test (66) following the ratio of 6:2:2.

4.2 Evaluation metrics

To evaluate how accurately the GFM predicts flood-susceptible regions compared with the simulation-based reference, we adopt three commonly used evaluation metrics inspired by [8]. All metric scores are scaled to a range of 0–100.

Hit Rate (HR). The HR corresponds to the *Recall* metric in a segmentation task. It measures the proportion of flood-risk pixels in the simulation data (F_s) that are correctly identified as flood-risk pixels by the GFM prediction (F_m). It is defined as:

$$HR = (F_m \cap F_s) / (F_s)$$

True Alarm Rate (TAR). Since HR alone does not penalize overprediction, we additionally use the TAR, which corresponds to *Precision* in segmentation tasks. Its value

Algorithm 1 Selection of TerraMesh Samples Based on FSM

Require: TerraMesh metadata, FSM raster
Ensure: List of TerraMesh sample keys

- 1: $C \leftarrow \text{ExtractCoordinates}(\text{TerraMesh_metadata})$
- 2: $G \leftarrow \text{CreateVectorGrid}(C)$
- 3: $(rp100, pwb) \leftarrow \text{ZoneStatistics}(G, \text{FSM_raster})$
- 4: **for** each grid $g \in G$ **do**
- 5: **if** $rp100_g < 1$ **or** $pwb_g < 1$ **then**
- 6: Remove g from G
- 7: **end if**
- 8: **end for**
- 9: $(rp100_{Q1}, pwb_{Q1}) \leftarrow \text{ComputeQuartileStats}(G)$
- 10: **for** each grid $g \in G$ **do**
- 11: **if** $rp100_g \leq rp100_{Q1}$ **and** $pwb_g \leq pwb_{Q1}$ **then**
- 12: Remove g from G and Continue
- 13: **end if**
- 14: Compute ratio $r_g \leftarrow pwb_g/rp100_g$
- 15: **if** $(r_g < 0.1$ **or** $r_g > 1)$ **then**
- 16: Remove g from G and Continue
- 17: **end if**
- 18: **end for**
- 19: **return** $\text{GetSampleKeys}(G)$

ranges from 0 to 1, where higher scores indicate fewer false positives and thus better model reliability. It is expressed as:

$$TAR = (F_m \cap F_s) / (F_m)$$

F1-Score (F1). For overall performance, we employ the F1 score, which is a more comprehensive measurement of true positives in the model outcome. This score is calculated from HR and TAR as follows:

$$F1 = 2(HR \times TAR) / (HR + TAR)$$

4.3 Training strategy

To evaluate the model under resource-constrained conditions, we fine-tune the GFMs using 186 training samples and employ Focal loss to address the class imbalance between foreground and background classes in the mask. The encoder components of the GFM architectures, *Prithvi*-v2.0 [26] and *TerraMind* [13], are kept frozen during fine-tuning, while a U-Net decoder is attached and trained to generate flood susceptibility masks. To prevent overfitting, we apply early stopping and select the model checkpoint that achieves the lowest validation loss. All experiments are conducted on a single NVIDIA A100 GPU node.

5 Results

We first evaluate the performance of flood susceptibility maps generated by different GFMs and input settings. While the *Prithvi* model supports only Sentinel-2 optical inputs, the *TerraMind* model was tested with both Sentinel-1 and Sentinel-2 inputs individually.

As summarized in **Table 1**, the *TerraMind* models using Sentinel-1 input outperform other configurations in terms

of F1 and TAR scores. In particular, the *TerraMind* model with Sentinel-1 input and the Thinking-in-Modality (TiM) mechanism achieved the highest performance, with F1 and TAR scores of 65.35 and 60.16, respectively.

Overall, the models tend to show relatively high HR (recall) but lower TAR (precision), suggesting that they capture most flood-prone regions but occasionally overestimate their extent. This pattern indicates that while the models are effective in identifying potential flood areas, future work should focus on improving boundary precision and reducing false alarms, potentially by integrating hydrological priors or spatial context from river network information.

Ablation study on TiM. We further analyze the impact of different TiM configurations using the *TerraMind*-large model with Sentinel-1 RTC input as the baseline.

As shown in **Table 2**, incorporating imaginary modalities yields consistent gains of approximately +0.8 pp in the average F1 score and +1.9 pp in the average TAR score. However, the HR score decreases across most TiM settings. Interestingly, when incorporating DEM and LULC as imaginary modalities, the model exhibits the opposite trend, increasing in HR by at least 6 pp, accompanied by a decrease of around 3 pp in both F1 and TAR scores.

These findings highlight that the TiM mechanism enhances the model’s capability under limited data conditions, although its effect varies depending on the choice of auxiliary modalities.

Input	Model	F1	HR	TAR
S2	Prithvi	60.18	62.55	55.23
	Prithvi-L	60.65	64.84	55.49
	TerraMind	60.86	65.23	55.66
	TerraMind-L	56.37	79.69	51.74
S1	TerraMind-TiM	56.67	68.18	54.56
	TerraMind-L-TiM	60.51	75.08	54.70
	TerraMind	63.11	<u>77.53</u>	56.82
	TerraMind-L	<u>64.77</u>	75.93	58.48
	TerraMind-TiM	64.15	<u>59.85</u>	60.16
	TerraMind-L-TiM	65.35	75.03	<u>59.16</u>

Table 1 Performance comparison of different Geospatial Foundation Model configurations. The acronyms “L” and “TiM” indicate large backbone size and the activation of the Thinking-in-Modality process, respectively. TiM settings depend on the model input (e.g., input: S2 corresponds to TiM: S1 + DEM + LULC). The best score in each column is shown in bold, and the second-best score is underlined.

6 Conclusion and Future Work

This paper presents ZeroFlood, a geospatial foundation model framework for data-efficient flood susceptibility mapping. By fine-tuning large Geospatial Foundation Models (GFMs) with Thinking-in-Modality (TiM) reasoning, ZeroFlood enables accurate predictions in data-scarce regions using minimal Earth Observation inputs. Exper-

TiM Setting	F1	HR	TAR
-	64.77 (-)	75.93 (-)	58.48 (-)
S2	66.50 (+1.73)	62.48 (-13.45)	63.49 (+5.01)
DEM	65.41 (+0.64)	71.67 (-4.26)	59.72 (+1.24)
LULC	66.60 (+1.83)	69.70 (-6.23)	61.51 (+3.03)
S2+DEM	<u>66.68 (+1.91)</u>	66.32 (-9.61)	<u>62.49 (+4.01)</u>
S2+LULC	67.21 (+2.44)	73.50 (-2.43)	61.42 (+2.94)
DEM+LULC	61.46 (-3.31)	82.31 (+6.38)	55.33 (-3.15)
S2+DEM+LULC	65.35 (+0.58)	75.03 (-0.90)	59.16 (+0.68)

Table 2 Experimental results for different Thinking-in-Modality configurations. The baseline model without TiM is shown in the first row, followed by models with other TiM settings and their performance differences relative to the baseline. The best score in each column is shown in bold, and the second-best score is underlined.

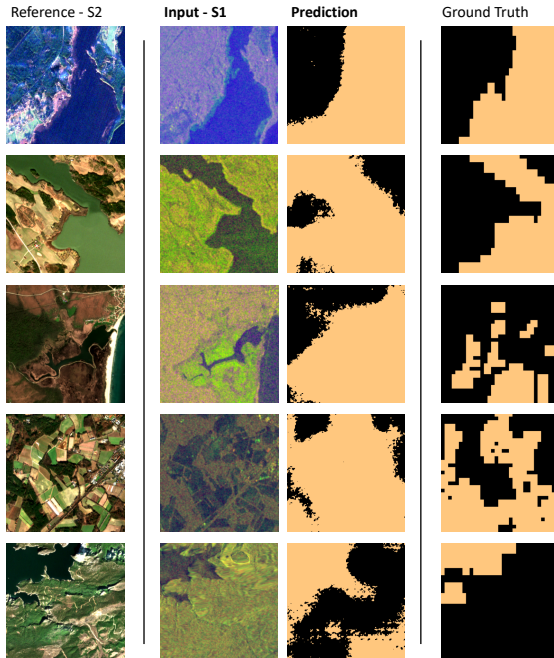


Figure 4 Representative examples of flood susceptibility predictions using the TerraMind-L-TiM model. The Sentinel-1 RTC input and the predicted mask are shown in the middle, while the Sentinel-2 L2A reference image and ground-truth mask are displayed on the left and right, respectively.

imental results showed that the TerraMind-Large model with Sentinel-1 input and TiM achieved the best overall performance, demonstrating that cross-modal reasoning enhances model robustness even in unimodal settings. Future research may incorporate hydrological priors and river-network information into GFM to improve spatial precision and reduce false-alarm rates. Another direction is to evaluate model generalization across unseen geographic regions and historical flood events for real-world transferability. Furthermore, the development of tiled or sliced inference strategies could extend local-scale predictions toward global flood susceptibility assessments. Collectively, these directions outline a path toward a more general and scalable paradigm for foundation model–driven flood risk analysis.

Acknowledgment

The work was made possible with the support of a scholarship from the German Academic Exchange Service (DAAD).

7 Literature

- [1] Albano R, Samela C, Crăciun I, Manfreda S, Adamowski J, Sole A, Sivertun Å, Ozunu A. Large scale flood risk mapping in data scarce environments: An application for Romania. *Water*. 2020 Jun 26;12(6):1834.
- [2] Aronsson-Storrier M. UN office for disaster risk reduction (2019). *YB Int'l Disaster L*. Online. 2021;2:377.
- [3] Baky MA, Islam M, Paul S. Flood hazard, vulnerability and risk assessment for different land use classes using a flow model. *Earth Systems and Environment*. 2020 Mar;4(1):225-44.
- [4] Blumenstiel B, Fraccaro P, Marsocci V, Jakubik J, Maurogiovanni S, Czerkawski M, Sedona R, Cavalilaro G, Brunschwiler T, Moreno JB, Longépé N. Terramesh: A planetary mosaic of multimodal earth observation data. In *Proceedings of the Computer Vision and Pattern Recognition Conference 2025* (pp. 2394-2402).
- [5] Cong Y, Khanna S, Meng C, Liu P, Rozi E, He Y, Burke M, Lobell D, Ermon S. Satmae: Pre-training transformers for temporal and multi-spectral satellite imagery. *Advances in Neural Information Processing Systems*. 2022 Dec 6;35:197-211.
- [6] Dionelis N, Fibaek C, Camilleri L, Luyts A, Bosmans J, Saux BL. Evaluating and benchmarking foundation models for earth observation and geospatial ai. *arXiv preprint arXiv:2406.18295*. 2024 Jun 26.
- [7] Dong S, Yu T, Farahmand H, Mostafavi A. A hybrid deep learning model for predictive flood warning and situation awareness using channel network sensors data. *Computer-Aided Civil and Infrastructure Engineering*. 2021 Apr;36(4):402-20.
- [8] Dottori F, Alfieri L, Bianchi A, Skoien J, Salamon P. A new dataset of river flood hazard maps for Europe and the Mediterranean Basin region. *Earth System Sci-*

ence Data Discussions. 2021 Jan 12;2021:1-35.

[9] Fereshtehpour M, Esmaeilzadeh M, Alipour RS, Burian SJ. Impacts of DEM type and resolution on deep learning-based flood inundation mapping. *Earth Science Informatics*. 2024 Apr;17(2):1125-45.

[10] Guo H, Liu Z, Jiang H, Wang C, Liu J, Liang D. Big Earth Data: A new challenge and opportunity for Digital Earth's development. *International Journal of Digital Earth*. 2017 Jan 2;10(1):1-2.

[11] Hashemi-Beni L, Gebrehiwot AA. Flood extent mapping: An integrated method using deep learning and region growing using UAV optical data. *IEEE Journal of Selected Topics in Applied Earth Observations and Remote Sensing*. 2021 Jan 14;14:2127-35.

[12] Hong D, Zhang B, Li X, Li Y, Li C, Yao J, Yokoya N, Li H, Ghamisi P, Jia X, Plaza A. SpectralGPT: Spectral remote sensing foundation model. *arXiv preprint arXiv:2311.07113*. 2023 Nov 13.

[13] Jakubik J, Yang F, Blumenstiel B, Scheurer E, Sedona R, Maurogiovanni S, Bosmans J, Dionelis N, Marsocci V, Kopp N, Ramachandran R. Terramind: Large-scale generative multimodality for earth observation. *arXiv preprint arXiv:2504.11171*. 2025 Apr 15.

[14] Li L, Xu T, Chen Y. Improved urban flooding mapping from remote sensing images using generalized regression neural network-based super-resolution algorithm. *Remote Sensing*. 2016 Jul 28;8(8):625.

[15] Li W, Lee H, Wang S, Hsu CY, Arundel ST. Assessment of a new GeoAI foundation model for flood inundation mapping. InProceedings of the 6th ACM SIGSPATIAL International workshop on AI for geographic knowledge discovery 2023 Nov 13 (pp. 102-109).

[16] Marsocci V, Jia Y, Bellier GL, Kerekes D, Zeng L, Hafner S, Gerard S, Brune E, Yadav R, Shibli A, Fang H. Pangaea: A global and inclusive benchmark for geospatial foundation models. *arXiv preprint arXiv:2412.04204*. 2024 Dec 5.

[17] Mehravar S, Razavi-Termeh SV, Moghimi A, Ranjgar B, Foroughnia F, Amani M. Flood susceptibility mapping using multi-temporal SAR imagery and novel integration of nature-inspired algorithms into support vector regression. *Journal of Hydrology*. 2023 Feb 1;617:129100.

[18] Nones M, Caviedes-Voullième D. Computational advances and innovations in flood risk mapping. *Journal of Flood Risk Management*. 2020 Dec 1;13(4).

[19] Patel DP, Ramirez JA, Srivastava PK, Bray M, Han D. Assessment of flood inundation mapping of Surat city by coupled 1D/2D hydrodynamic modeling: a case application of the new HEC-RAS 5. *Natural Hazards*. 2017 Oct;89(1):93-130.

[20] Prasad P, Loveson VJ, Das B, Kotha M. Novel ensemble machine learning models in flood susceptibility mapping. *Geocarto International*. 2022 Aug 18;37(16):4571-93.

[21] Reed CJ, Gupta R, Li S, Brockman S, Funk C, Clipp B, Keutzer K, Candido S, Uyttendaele M, Darrell T, Scale-mae: A scale-aware masked autoencoder for multiscale geospatial representation learning. InProceedings of the IEEE/CVF International Conference on Computer Vision 2023 (pp. 4088-4099).

[22] Rentschler J, Salhab M. People in Harm's Way. *Flood Exposure and Poverty* in. 2020 Oct;189.

[23] Sampson CC, Smith AM, Bates PD, Neal JC, Alifieri L, Freer JE. A high-resolution global flood hazard model. *Water resources research*. 2015 Sep;51(9):7358-81.

[24] Seydi ST, Kanani-Sadat Y, Hasanlou M, Sahraei R, Chanussot J, Amani M. Comparison of machine learning algorithms for flood susceptibility mapping. *Remote Sensing*. 2022 Dec 29;15(1):192.

[25] Sidek LM, Jaafar AS, Majid WH, Basri H, Marufuzzaman M, Fared MM, Moon WC. High-resolution hydrological-hydraulic modeling of urban floods using InfoWorks ICM. *Sustainability*. 2021 Sep 14;13(18):10259.

[26] Szwarcman D, Roy S, Fraccaro P, Gíslason PE, Blumenstiel B, Ghosal R, de Oliveira PH, Almeida JL, Sedona R, Kang Y, Chakraborty S. Prithvi-eo-2.0: A versatile multi-temporal foundation model for earth observation applications. *arXiv preprint arXiv:2412.02732*. 2024 Dec 3.

[27] Tellman B, Sullivan JA, Kuhn C, Kettner AJ, Doyle CS, Brakenridge GR, Erickson TA, Slayback DA. Satellite imaging reveals increased proportion of population exposed to floods. *Nature*. 2021 Aug 5;596(7870):80-6.

[28] Wang Y, Braham NA, Xiong Z, Liu C, Albrecht CM, Zhu XX. SSL4EO-S12: A large-scale multimodal, multitemporal dataset for self-supervised learning in Earth observation [Software and Data Sets]. *IEEE Geoscience and Remote Sensing Magazine*. 2023 Sep 25;11(3):98-106.

[29] Wei J, Wang X, Schuurmans D, Bosma M, Xia F, Chi E, Le QV, Zhou D. Chain-of-thought prompting elicits reasoning in large language models. *Advances in neural information processing systems*. 2022 Dec 6;35:24824-37.

[30] Xiong Z, Wang Y, Zhang F, Stewart AJ, Hanna J, Borth D, Papoutsis I, Le Saux B, Camps-Valls G, Zhu XX. Neural plasticity-inspired foundation model for observing the earth crossing modalities. *CoRR*. 2024 Jan 1.

[31] Zarzar C, Siddique R, Hosseiny H, Gomez M. Quantifying uncertainty in flood inundation mapping using streamflow ensembles and hydraulic modeling techniques. *Natl. WATER Cent. Innov. Progr. SUMMER Inst. Rep.* 2016 Oct 20;4:71.

[32] Zhu Z, Wulder MA, Roy DP, Woodcock CE, Hansen MC, Radeloff VC, Healey SP, Schaaf C, Hostert P, Strobl P, Pekel JF. Benefits of the free and open Landsat data policy. *Remote sensing of environment*. 2019 Apr 1;224:382-5.